

**Review of Aeronautical Fatigue**  
**Investigations in Switzerland**

March 2019 – April 2021

*Swiss National Review*  
*of the International Committee on Aeronautical Fatigue and*  
*Structural Integrity*

*Conference and Symposium postponed due to COVID-19*

*June 2021 Webinar*



## Document: ZAV-KOR2021-001

**Prof. Dr. Michel Guillaume**  
**Zurich University of Applied Sciences**  
**ZHAW / School of Engineering**  
**Centre for Aviation**

Zurich University  
of Applied Sciences



### Summary

This document reviews the work that has been done in Switzerland in the field of aeronautical fatigue. Contributions to the document were made by Zurich University of Applied Sciences (ZHAW), Lucerne University of Applied Sciences and Arts (HSLU), RUAG AG (RUAG), and the Swiss Federal Laboratories for Materials Science and Technology (Empa). This document represents a chapter of the ICAF National Reviews document that is published online on the ICAF website. The format of the review conforms to ICAF requirements.

Prepared and approved for the presentation for ICAF website [www.icaf.aero](http://www.icaf.aero)

## Table of Contents

<b>Summary .....</b>	<b>- 2 -</b>
<b>4.1 Introduction .....</b>	<b>- 4 -</b>
<b>4.2 Swiss Aviation Activities .....</b>	<b>- 4 -</b>
<b>4.3 Ageing Airplanes (Pilatus P3, Hunter Mk58/68) .....</b>	<b>- 9 -</b>
<b>4.4 Activities Hochschule Luzern (HSLU).....</b>	<b>- 12 -</b>
<b>4.5 F/A-18 Inner Wing Inboard TEF Hinge: Crack Growth Investigations .....</b>	<b>- 14 -</b>
<b>4.6 Fatigue Monitoring &amp; Individual A/C Tracking based on Nz Exceedance Data .....</b>	<b>- 20 -</b>
<b>4.7 TSA Fatigue Evaluation .....</b>	<b>- 23 -</b>
<b>4.8 Development and operation of two test benches for the evaluation of a structural health monitoring system.....</b>	<b>- 27 -</b>

## 4.1 Introduction

The present review gives a brief summary of the work performed in Switzerland in the field of aeronautical fatigue in the period from April 2017 to March 2019. Contributions were made by the following organisations:

- Zurich University of Applied Sciences (ZHAW); Centre for Aviation of the School of Engineering
- Lucerne University of Applied Sciences and Arts (HSLU); Department of Engineering and Architecture
- Gottier Engineering GmbH
- Swiss Federal Laboratories of Materials Science and Technology (EMPA)
- RUAG AG, Emmen; Department of Structural Engineering

The many interesting contributions are gratefully acknowledged, especially the effort of Xinying Liu (ZHAW), Markus Gottier (Gottier Engineering), Silvain Michel (EMPA), Dejan Romančuk (HSLU), and Andreas Uebersax (RUAG AG).

The financial support by the Swiss Federal Office of Civil Aviation (FOCA) is gratefully acknowledged for the activities of the Ageing Aircraft project. Personal thanks to Mr. Hamid Hampai from FOCA for supporting the project and the Zurich University of Applied Sciences, ZHAW in Winterthur. armasuisse is acknowledged for the supervision and funding of work carried out for military aircraft in RUAG AG.

## 4.2 Swiss Aviation Activities

Zurich University of Applied Sciences, Michel Guillaume

2019 was a good year for the Swiss aviation industry, which saw the successful certification of the Pilatus PC-12 NGX (Figure 4. 1) in October 2021 with the PT6E engine. The PC-12 NGX features new propellers and wider windows for more comfort. The noise inside cabin and out was further reduced and performance was again improved. The avionics were upgraded to provide additional safety. The maintenance interval (TBO) could be doubled to 600 hours. All these measures combined contribute to the ongoing success of the Pilatus PC-12, promising interesting future opportunities.



Figure 4. 1: PC-12 NGX

In Januar 2021 Pilatus was able to deliver the 100<sup>th</sup> PC24 versatile business jet. Production for 2021 has already soled out, underscoring the success of Pilatus inspite of the COVID-19 crisis. The PC-24 has also been certified for short and light field performance, which provides a major advantage compared to other business jets. The Australian Royal Flying Doctor Service is one of the first operators in rough fields, see Figure 4. 2.

In general though, it is safe to sy that the Swiss aviation industry has been hard hit by the Covid-19 crisis. Airports, airlines and suppliers are still far off from recovery. As it becomes more apparent that there will not be a quick recovery from this crisis, it is becoming increasingly unavoidable that there will be layoffssaccross the industry, that will have a lasting knock-on affect on the aviation sector.



Figure 4. 2: Pilatus PC-24 operated by Royal Flying Doctors in Australia

The innovative Swiss SH 90 helicopter made some progress in its certification process. The helicopter was developed from scratch, including the airframe (fully composite), rotor head with gear and blades. The kopter group has made a big effort, particularly given that time is running and customers are eagerly waiting certification. In April 2020 the Leonardo group acquired the kopter group and included the revised SH 90 helicopter in their portfolio. The goal of Leonardo is to run the former kopter group as research center for sustainable development. The rotor head was replaced by a Leonardo product and flight testing resumed, see Figure 4. 3.



Figure 4. 3: Revised Leonardo kopter Sh 90 helicopter in flight

Switzerland has yet to introduce the new EU drone regulation, which is pending due to a referendum launched by the Swiss model plane association. Progress was made with first services launched by air navigation service provider Skyguide for Swiss unmanned traffic management called Swiss U-Space. Swisscom is providing a remote identification device which transmits data via the 4G mobile network in connection with FARM and ADSB data for anti collision.

Switzerland is well known as the Home of Autonomous Systems. There are a lot of start ups developing drones for various applications with sophisticated sensor integrations. Also urban air mobility concepts are in an early detailed design phase. The most popular is the concept of Dufour Aerospace, for which wind tunnel tests and simulations are underway to define the first prototype, see Figure 4. 4. The hybrid propulsion integration, with all the performance, reliability and maintainability aspects, is challenging in this EVTOL concept.



Figure 4. 4: Early concept of Dufour Aerospace EVTOL concept

The final report of the crash of the Junkers Ju-52 in August 2017 was released by SUST, the Swiss transport safety investigation board. All three crew members and 17 passengers were killed. The direct cause of the accident was attributed to the fact that, after losing control of the aircraft, there was insufficient space to regain control of the aircraft, which then crashed into the ground, see Figure 4. 5. The investigation identified the following contributing factors:

- The flight crew was accustomed to not complying with the recognized rules for safe flight operations and taking high risks during flights in the area of Piz Segnas.
- The aircraft involved in the accident was operated with a centre of gravity position that was beyond the rear limit.

Due to the age of the aircraft, built in 1936, the structure of the wreckage was analysed in detail. They observed some corrosion and small cracks in wing spar locations. The cracks did not show any critical crack length. But the maintenance was also criticized for not being done as it should have been according to the Part 145 maintenance organization. Currently, a new company called Junkers Flugzeugwerke AG is doing reverse engineering to build a new replica of the original Junkers Ju-52. The goal is to certify the replica and offer public flights again.

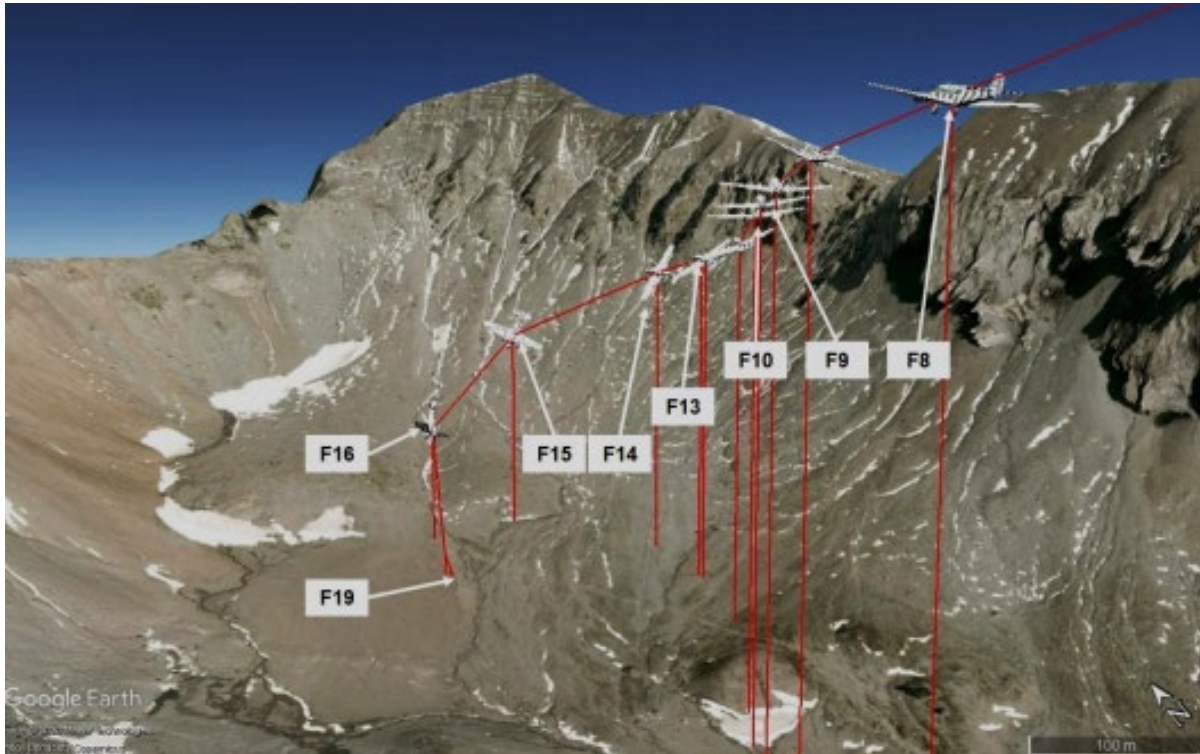


Figure 4. 5: Reconstruction of the final flight path of Ju-52 into the ground

In 2019 the Swiss Federal Authority for Civil Aviation FOCA started a project focusing on air space and aviation infrastructure (AVISTRAT-CH). Switzerland already has one of the most complex air space structures, which will be even more complex with the introduction of new players such as drones and urban air mobility vehicles. In order to address the problem, all stakeholders were involved to develop a high level vision for 2035. New strategic pillars were provided by three architects; Oliver Wyman Group, NLR from the Netherlands and the Aviation Research Center Switzerland (ARCS). The strategy should focus on sustainability, regulation, safety, and the economy. The three proposals of the architects will be evaluated by the end of summer to define a unique Swiss strategy for the air space and aviation infrastructure to be implemented by 2035.

The evaluation of a new fighter for the Swiss Air Force to replace the F5 Tiger and the F/A-18 Hornet is in the final stages, after passing a referendum successfully, by a narrow majority, for the acquisition of the new fighters. The decision on who the tender is awarded to will be communicated late in summer 2021.

### 4.3 Ageing Airplanes (Pilatus P3, Hunter Mk58/68)

Gottier Engineering GmbH, Markus Gottier; Zurich University of Applied Sciences, Michel Guillaume

#### **Pilatus P3**

In 2012 an Ageing Program for different historical aircraft registered in Switzerland was initiated by the Swiss Federal Office of Civil Aviation (FOCA) in order to get a better overview of the structural integrity of these aircraft. Several investigations and analyses were started. The goal was to obtain more information for a future Supplemental Structural Inspection Document (SSID). The purpose of this document is to define specific inspections to prevent any potential structural failures early in time. With regard to the Pilatus P3 a supplemental inspection program was started a few years ago. Several activities (see below) were necessary in order to get enough information to establish a P3 specific SSID:

- Structural analysis of the aircraft and verification of available structural reports
- Special inspection of the fleet leader aircraft (HB-RCH)
- Identification of the critical structural locations
- Development of a typical load model and determination of specific load spectra
- Performing of several Crack Growth (CG-) analyses
- Producing a structural integrity report based on the above mentioned steps

All these activities were performed by the “Zürcher Hochschule für Angewandte Wissenschaften” (ZHAW) in collaboration with FOCA and the Associazione RCH (owner and operator of the fleet leader aircraft HB-RCH). As a result of that a P3 SSID has been issued. It contains informations and recommendations for P3 owners to perform the necessary supplemental inspection tasks which are required for a safe operation of the P3 aircraft.

Following 4 locations (see Figure 4. 6) have been identified as the most critical parts from the point of view of the structure integrity. These parts are called Fracture and Fatigue Critical Structures (FFCS): HTL-Fitting (1); External Wing Splice at rib 12 (2); Internal Wing Splice at rib 12 (3); Upper fuselage attachment (4). Detailed Crack Initiation (CI-) and Crack Growth (CG-) analyses have been performed for these parts.

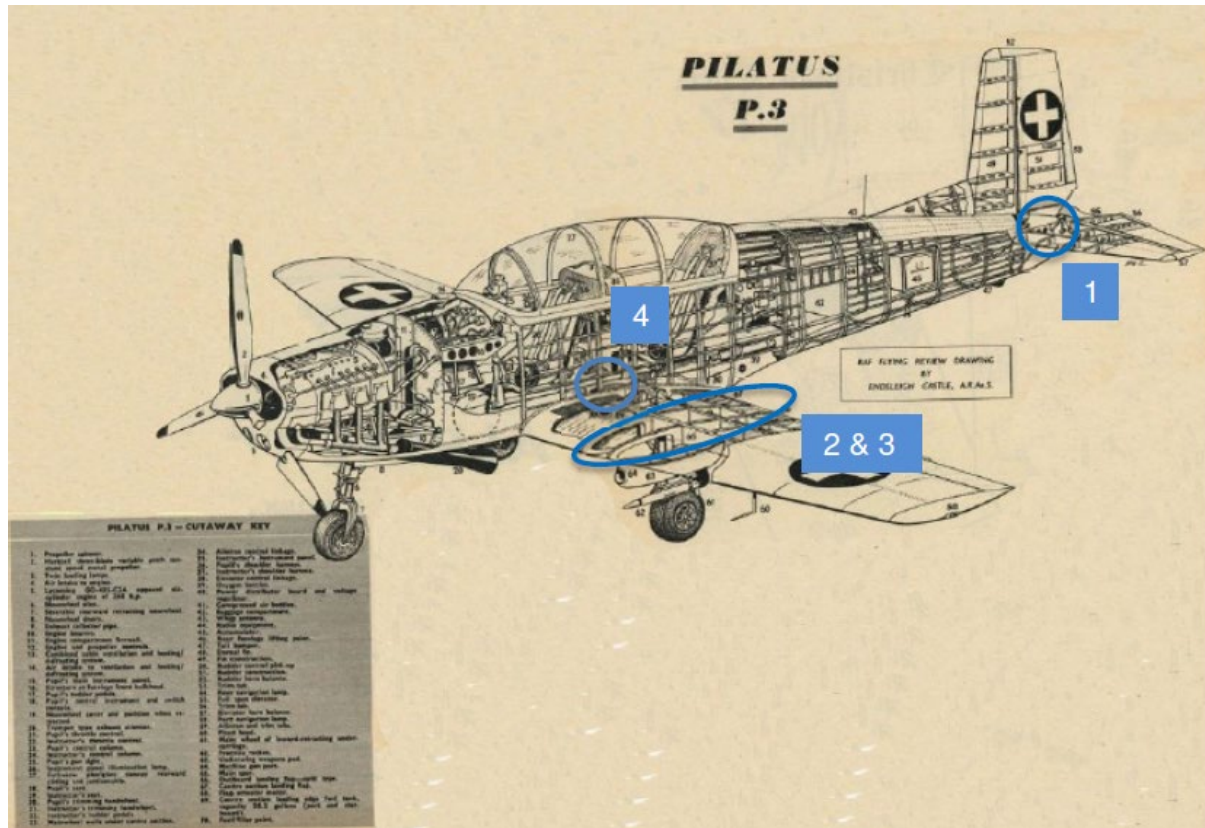


Figure 4. 6: Fracture and Fatigue Critical Structures (FFCS)

Additional critical locations from the fatigue point of view exist in the structure of the P3 aircraft. These are mainly hole-lugs of hinges of the ailerons, the elevator and the rudder. They are called Fatigue Critical Structure parts (FCS).

Since these parts may be affected by the same problem as the HTL fitting (location 1 in Figure 4. 6) a comparison of each FCS part with the HTL fitting was made from the point of view of lug stress and geometry. It appears that each FCS part is less critical than the reference location; i.e. the HTL fitting. The SSID contains also information about Corrosion Inspections. The basis for these inspections is the result from the fleet leader corrosion inspections carried out in 2015. Since almost no corrosion damages were discovered on this aircraft the defined corrosion inspections in the standard Aircraft Maintenance Program remain valid. Thus no specific additional corrosion inspection was considered to be addressed in the P3 SSID.

### Hunter Mk58/68

As part of the Civil Aviation Maintenance Program of the Hunter Mk58/68 a NDI check has been performed on the front wing to fuselage attachment fitting. In this process cracks has been discovered on the upper and the lower side of the fitting radius (see Figure 4. 7). It is to mention that this kind of cracks have already been discovered in the past on the Hunter Mk58/68 aircraft.

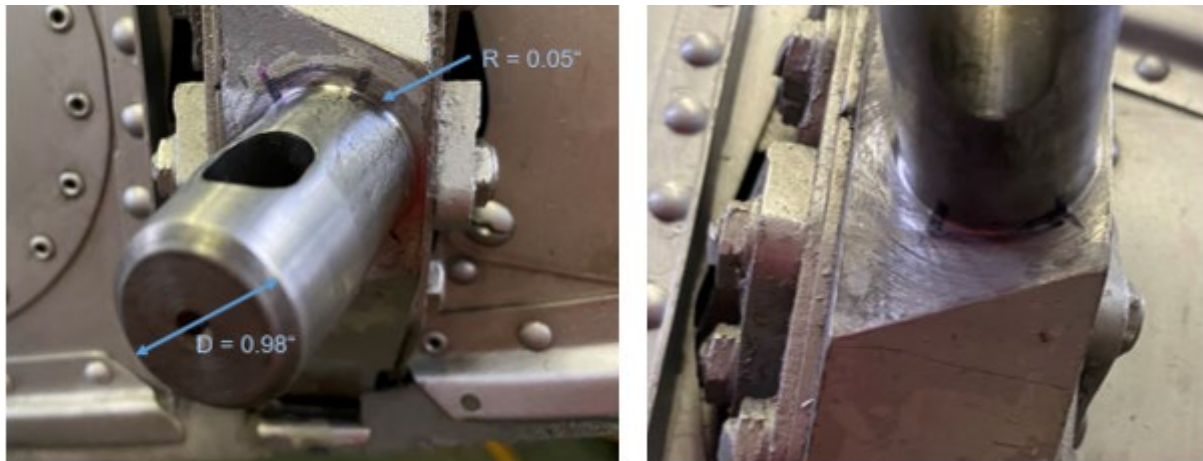


Figure 4. 7: Cracks in the radius on the upper (LH) and lower (RH) side of the front attachment fitting

In order to assess the criticality of these cracks a crack initiation (CI) and crack growth analyses have been carried out. The biggest challenge of these analyses was to define the fitting loads and their spectra; neither fitting loads nor loads spectra were actually known.

Due to the lack of these data following conservative assumptions were made:

- The material of the fitting is a AISI 4330 steel with a tensile strength of  $F_{tu} = 1'450$  MPa. It is assumed that the nominal stress is  $\sigma_{limit} = 967$  MPa ( $= 1'450$  MPa/ 1.5) at the limit load of  $n_z = 7.5$  g. Since the actual maximum usage of the Hunters Mk68T aircraft is limited to 5.5g it results a max nominal stress at 5.5 g of  $\sigma_{max} = 709$  MPa.

Note : the actual usage of this aircraft was monitored during one year.

- The FALSTAFF sequence containing 35'966 peaks and valleys and representing 200 flights was used. Since cracks of the same size were discovered on both sides of the fitting radius it was assumed that a symmetrical spectrum exists. Thus the FALSTAFF spectrum was flipped and added to the normal sequence. As a result of that the modified sequence consists of a normal and a flipped FALSTAFF sequence containing 71'932 peaks and valleys. Conservatively it is assumed that this sequence still represents 200 flights.

Based on these conservative assumptions a crack initiation analysis based on the Neuber-Notch approach was performed. It resulted a very short CI-life of 800 flights. This was already expected for the 0.05" (1.25mm) root radius.

The CG analysis was carried out with the same stress and spectrum assumptions . The initial crack size was the detected crack size at the inspection, i.e. 0.403" (10.3mm ) length and 0.082" (2.1mm) depth. The crack growth curve is shown in Figure 4. 8. The crack growth life is 4000 flights. This is by far longer than the 25 flights, which is authorized by the Swiss Federal Office of Civil Aviation.

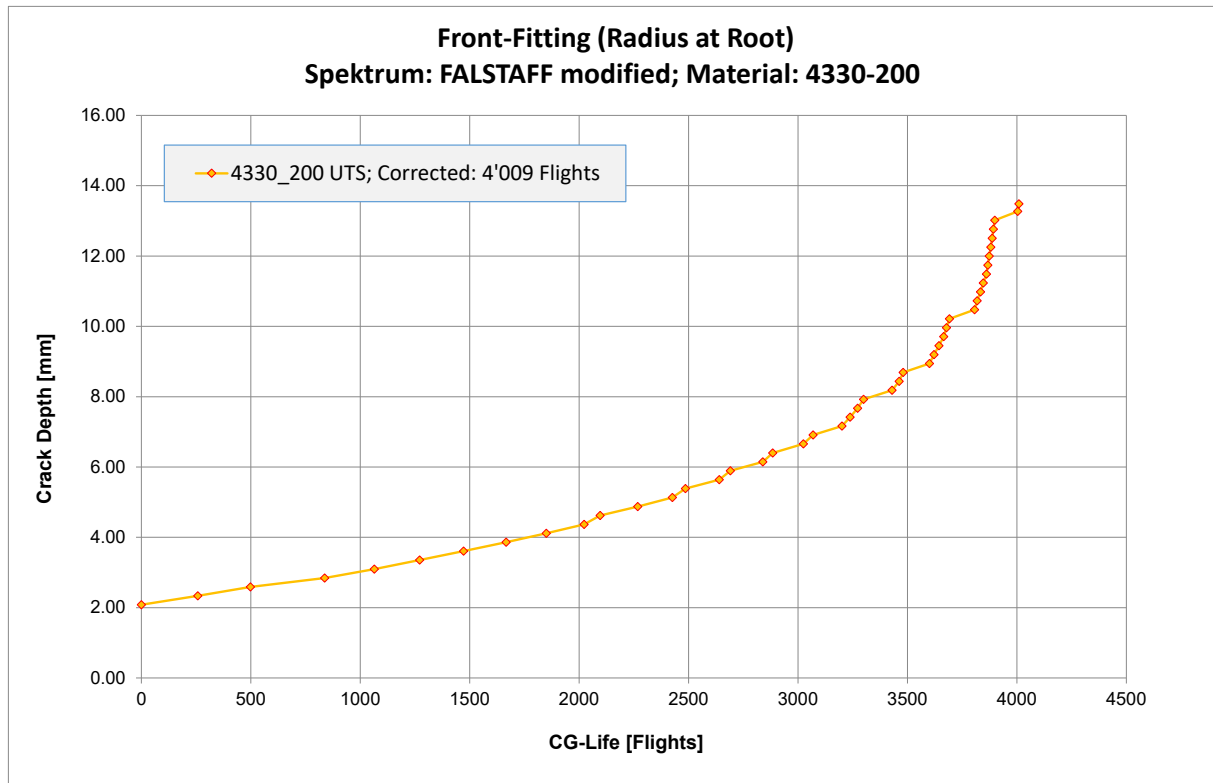


Figure 4. 8: Crack growth life of front attachment fitting

## 4.4 Activities Hochschule Luzern (HSLU)

Lucerne University of Applied Sciences and Arts, Dejan Romančuk

Activities in aeronautical structural integrity at the Lucerne University of Applied Sciences and Arts (Hochschule Luzern - HSLU) are carried out at the Institute of Mechanical Engineering and Energy Technology (IME). In the following, related projects as part of applied research programs or engineering services are outlined.

Aircraft skin panel dents resulting from foreign object damages or other accidental damages require instructions for continued airworthiness. These may include leave as-is, dress-out, doubler repair or skin replacement dispositions depending on the size and location of damage. For optimized in-service actions the current dent allowables and substantiation methodology for Pilatus Aircraft are being revisited. A coupon test program on dented and pre-cracked skin aluminum sheets is being performed and the crack growth behavior is investigated based on image processing technology. The effects of dent damages on the crack growth behavior are being studied for various parameters.

Metallic additive manufacturing (AM) offers many advantages for design or maintenance organizations in the aircraft industry, however, qualification and certification challenges are demanding. A so called defect tolerant AM research project was initiated. It supports the extension of the AM process to load-carrying, safety-relevant components, i.e. to durability critical elements or principal structural elements, respectively. The design of metallic AM parts poses challenges, especially due to intrinsic imperfections. Adequate design methods in combination with quality assurance measures should ensure structural integrity while the extensive qualification testing is to be minimized. Non-recurring certification, qualification and including delta qualification costs (e.g. when changing production machines) are considered as show stoppers for a business case. Enabling better access to this manufacturing process for smaller design organizations requires clear design methodologies and a predictable path to qualification and certification.

A research tool-box has been built to test the feasibility of the proposed structural integrity concept: Fabrication of specimens from the metallic 3D printer, determination of fatigue strength, application of X-ray imaging using computed tomography (CT) to identify discontinuities, models and software for quantification and characterization, fabrication of flaws to study crack propagation behavior, etc. Intrinsic flaws were successfully identified, visualized, and processed using the CT scanner. The fatigue behavior of specimens, which were made from titanium powder, shall be correlated with the distribution and nature of the discontinuities. This will allow statements on strength based on CT scans only and thus merge design and quality criteria.

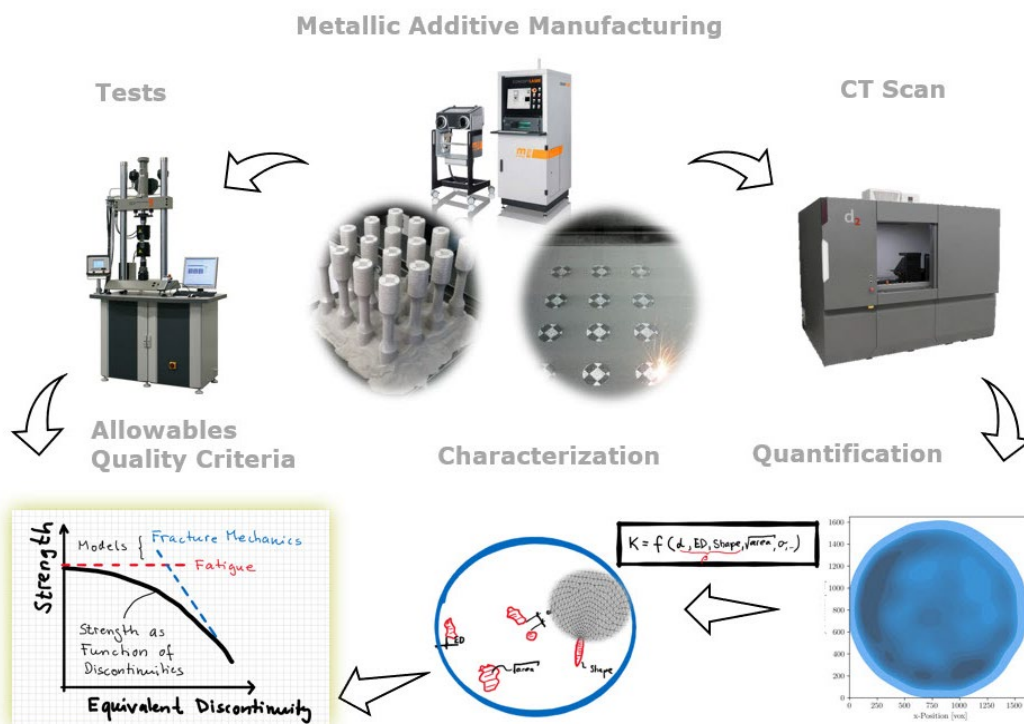


Figure 4. 9: Design Allowables and Quality Acceptance Criteria Concept for Additive Manufacturing

In collaboration with Dr. Juan Ocampo, St. Mary's University, San Antonio, case studies for quantitative structural risk assessment of aging swiss air force fleet were developed and discussed to improve and expand current methodologies. In this context, participation with the holistic structural integrity process (HOLSIP) network was valuable. HOLSIP is based on the fundamental idea that failure modes or mechanisms are interconnected, and it is a physics based design approach that is the underpinning of a reliability and integrity centered design system.

Future HSLU activities will focus on the above mentioned fields and i in the field on non-destructive inspections for AM and structural health monitoring.

## 4.5 F/A-18 Inner Wing Inboard TEF Hinge: Crack Growth Investigations

RUAG AG, G. Cassina, R. Rigoli, T. Stehlin, R. Zehnder

The F/A-18 Inner Wing (IW) Trailing Edge Flap (TEF) Inboard Hinge is one of the two attachment points of the TEF. The forward flange attachment holes, connecting the TEF hinge to the lower surface of the wing, are known critical locations. Fatigue cracks have been reported by many F/A-18 operators. Conducted studies identified the root cause for the cracking as a combination of bearing loads and local bending effects induced by the high fastener tension loads.

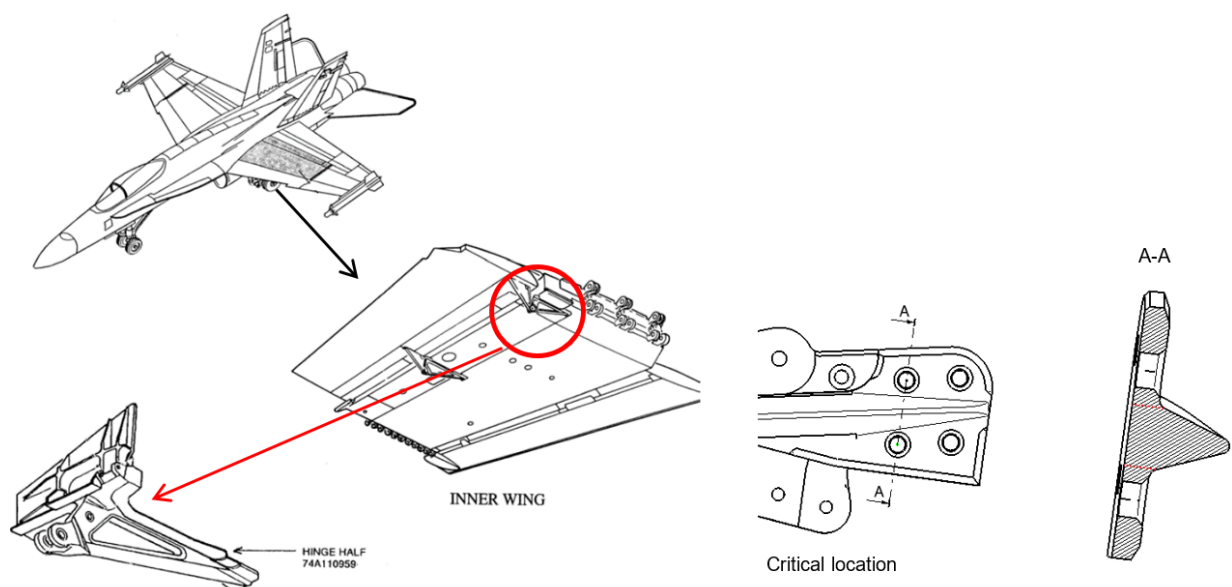


Figure 4. 10: Position of IW TEF TEF hinge (left) and critical holes (right)

During inspections, a cracked TEF hinge has been detected. The cracked TEF hinge has been replaced and the cracked area has been made available for quantitative fractography (QF1) investigations. RUAG AG used the QF data of the cracked holes (Figure 4. 11) to develop and validate a crack growth (CG) model of the TEF hinge cracking.

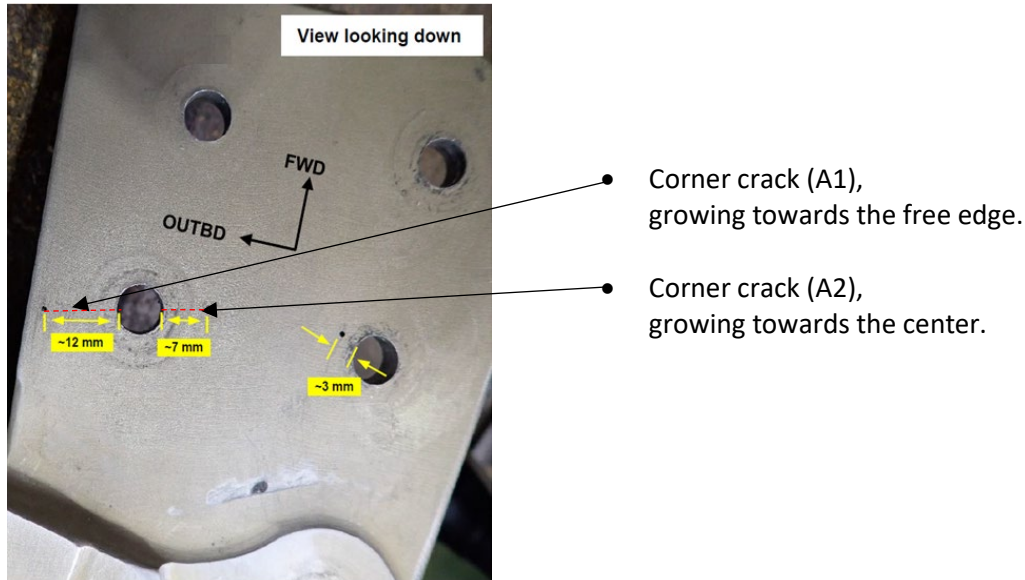


Figure 4. 11: Position of Crack used for QF investigations

### QF results

QF evaluation of the cracked hole propagating towards the free edge was able to identify a 0.00165" (0.042 mm) indentation as probable crack origin. The image of the crack is presented in Figure 4. 12. Along the hore surface (a-length), the crack has grown about 1.0 mm beyond the edge of the countersunk. Along the surface (c-length) the length is about 12.0 mm.

The analysis of the fracture surface of the crack growing towards the hinge centerline identified a damage, probably caused by the drill during manufacturing. Furthermore, a 0.00177" (0.045 mm) defect was also observed at the edge of the hole. Both could have acted as Equivalent Pre-Crack Size (EPS). The length along the faying surface (C-length) is about 0.227" (5.78 mm), the one along the bore hole (A-length) 0.133" (3.38 mm), see Figure 4. 13.

<sup>1</sup> Ref.: Engineering Failure Analysis, Volume 96, February 2019, Pages 426-435

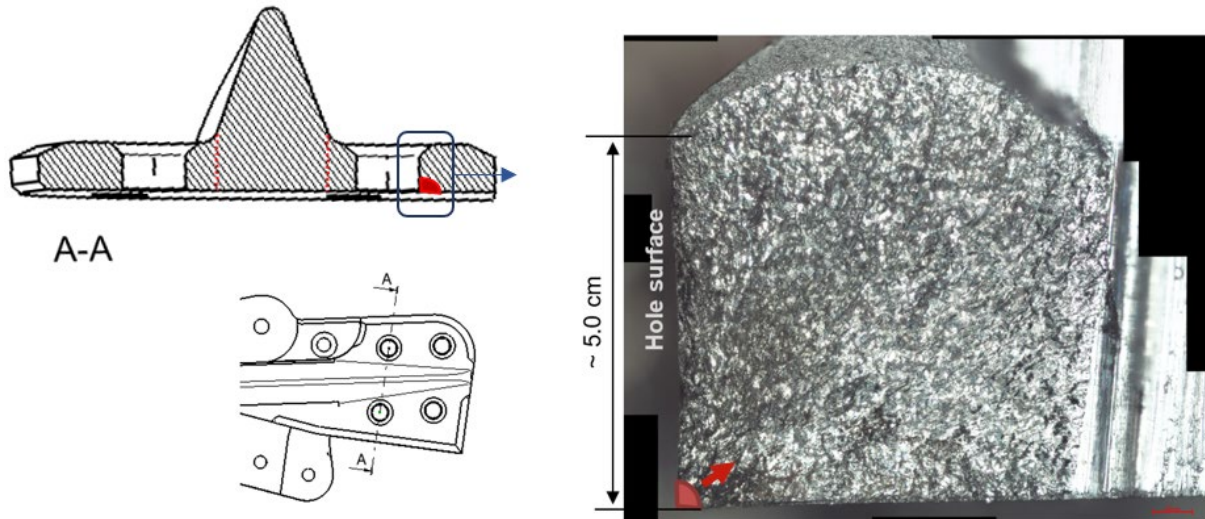


Figure 4. 12: Corner crack (A1), growing towards the free edge

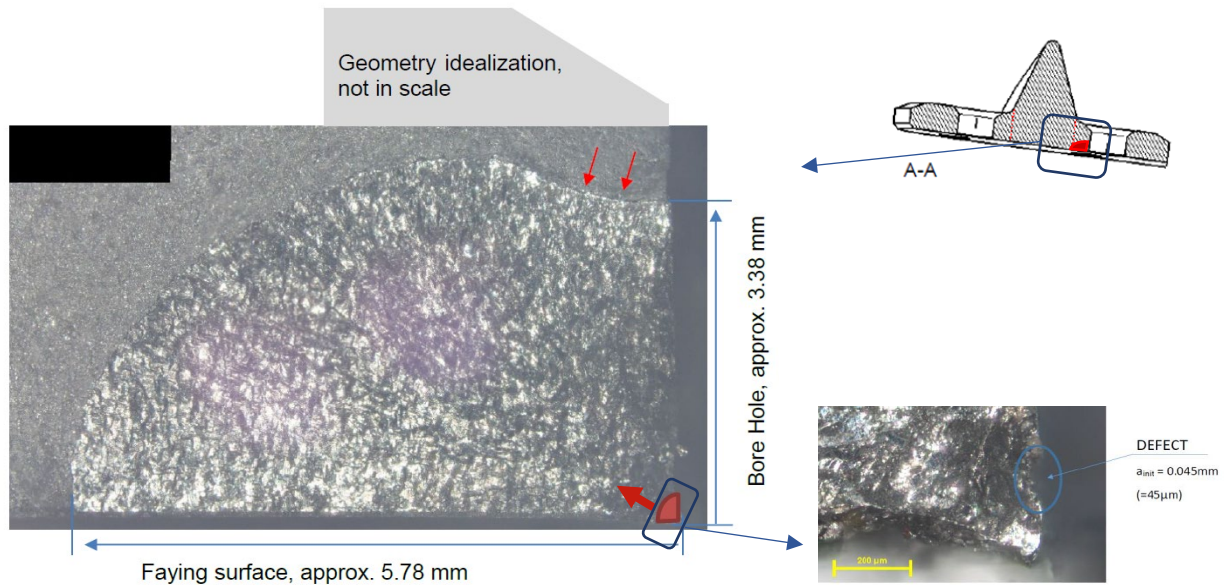


Figure 4. 13: Corner crack (A2) growing towards the center

The crack growth is affected by local effects below the countersunk head of the fastener. Along the bore hole, in the upper region (marked by the red arrows), the crack has slowed down. This can also be observed by the change in the CG curve slope presented later on.

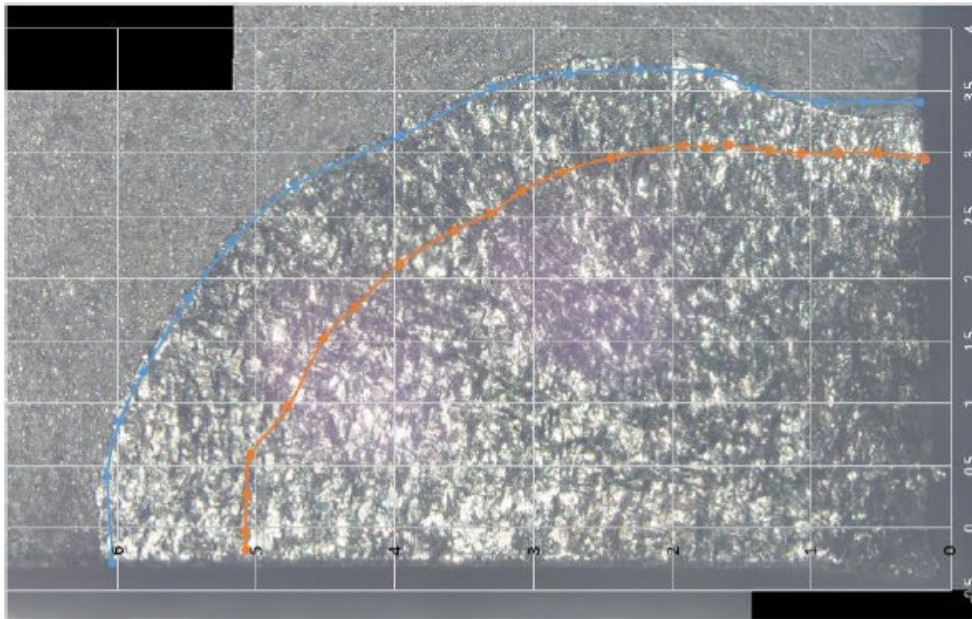


Figure 4. 14: Crack front (A2) towards hinge center, different lengths along bore hole

As the crack growth rate is not constant along both directions, the crack shape can be approximated by an ellipse with an aspect ratio of about 1.0 to 1.7.

### CG Model

Loads for the crack growth analysis are extracted from a detailed FEM of the IW area around the hinge. An existing Nastran FE model, reproducing the inner portion of the inner wing of the F/A-18, has been refined and modified by introducing linear gaps around the periphery of the horizontal flange of the TEF hinge to account for the heeling and toeing effect between the TEF hinge and the surrounding structure.

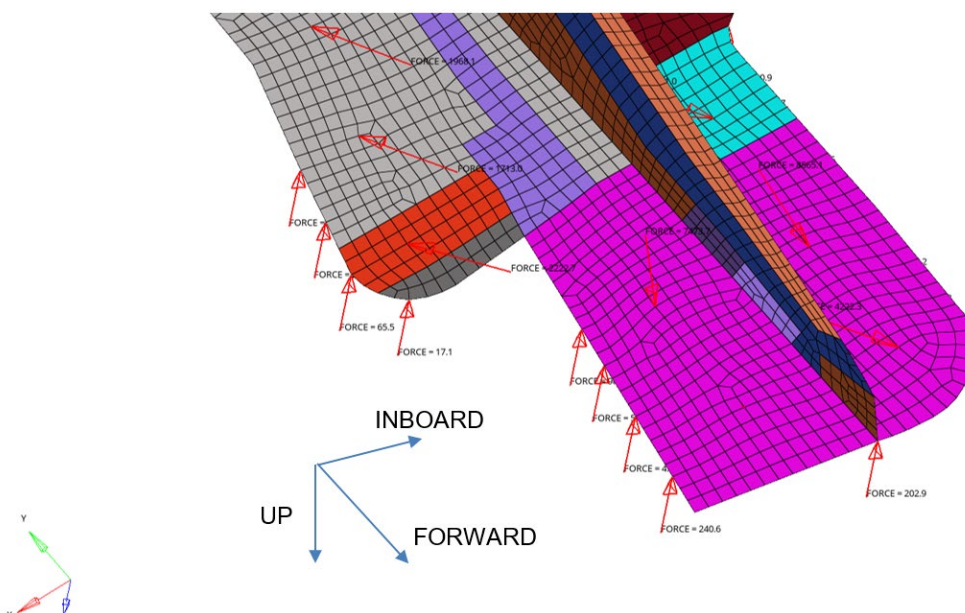


Figure 4. 15: Detail of FEM mesh at TEF hinge forward flange

Two CG model scenarios have been investigated:

- Scenario 1: SC01\_G01, Corner crack at hole (A1), growing towards the free edge.
- Scenario 2: SC02\_G01, Corner crack at hole (A2), growing towards the center.

CG analyses are performed with AFGROW using advance model solutions. Loads extracted from the FE model, found to be in line with the findings, are used to derive the local loading at hole (A1), which has been identified as the most critical. Through stress, bending stress and bearing stress are computed by performing a local load split in an area of approximately  $4D$  around the hole center.

Using Mohr's circle equations, the loads are used to obtain an equivalent gross stress at different angles around the hole. The crack plane is defined as the direction which maximizes the equivalent gross stress.

Stress gradients along the section width due to in-plane bending (section lateral bending) are also derived from the FEM data and are used to develop stress intensity correction solution (Beta correction) for the AFGROW analysis.

The setup of the crack growth models in AFGROW is presented in Figure 4. 15. The geometry of the TEF hinge flange required to be idealised by neglecting the triangular section and by neglecting the fastener countersunk.

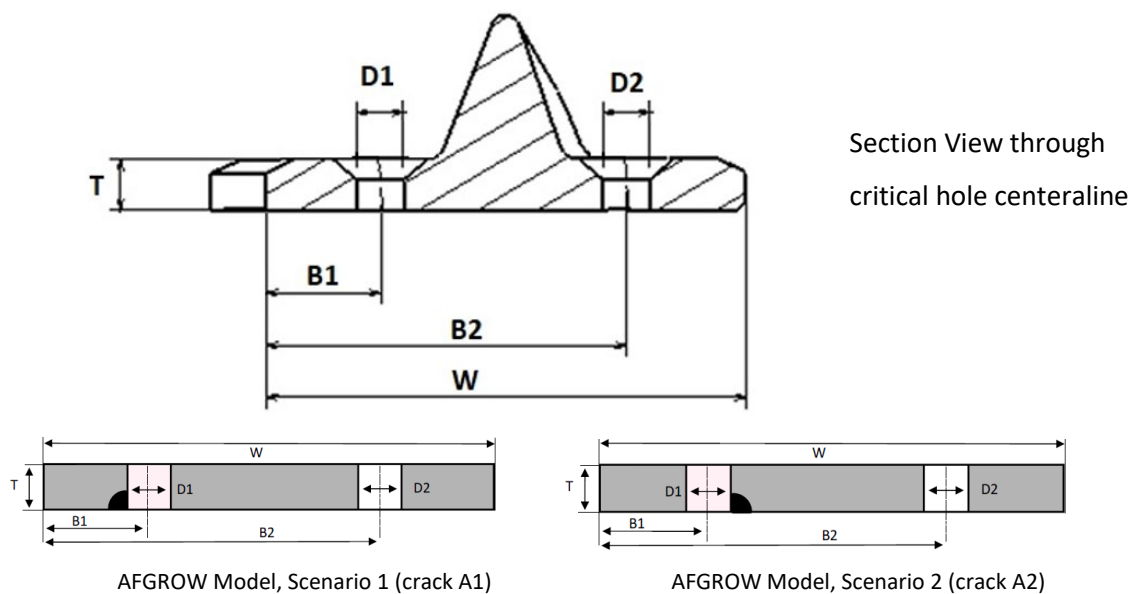


Figure 4. 16: AFGROW crack growth models

QF data of the cracked hinge is used to validate the CG models. A good match between observations and AFGROW model predictions is observed for both CG scenarios.

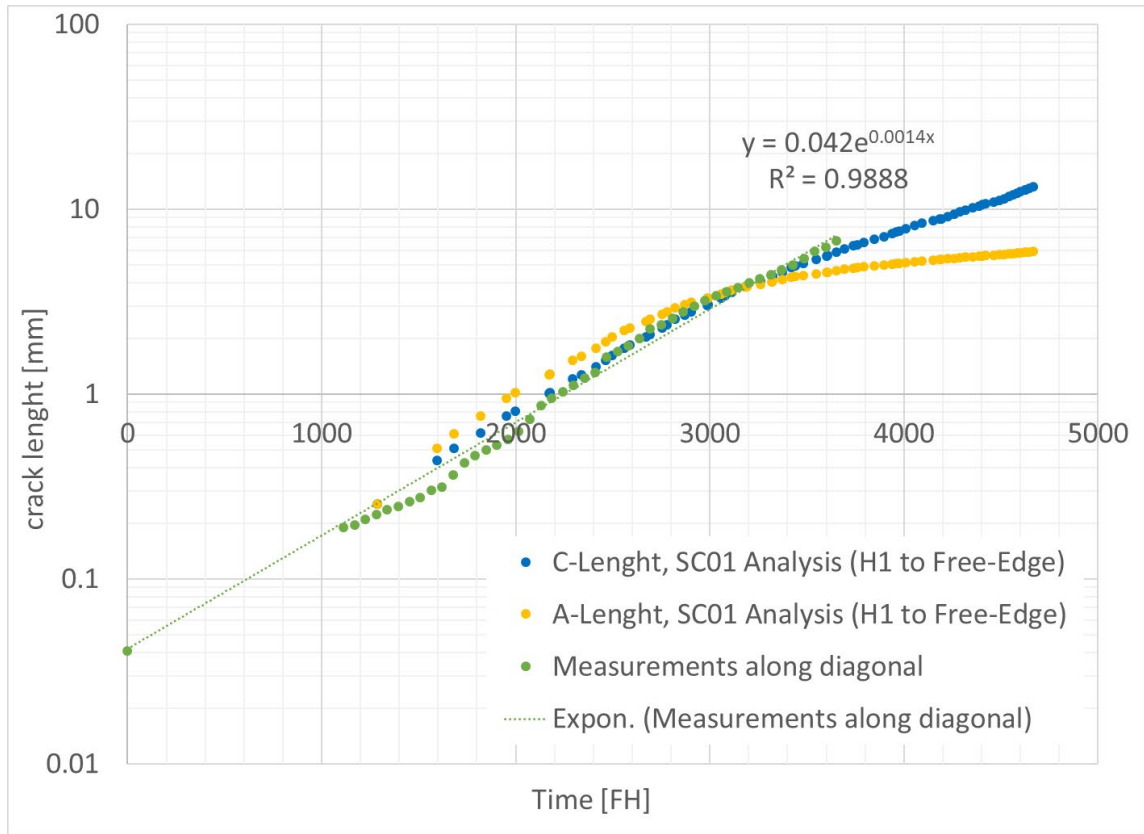


Figure 4. 17: AFGROW predictions vs. measurements, crack hole (A1) towards free edge

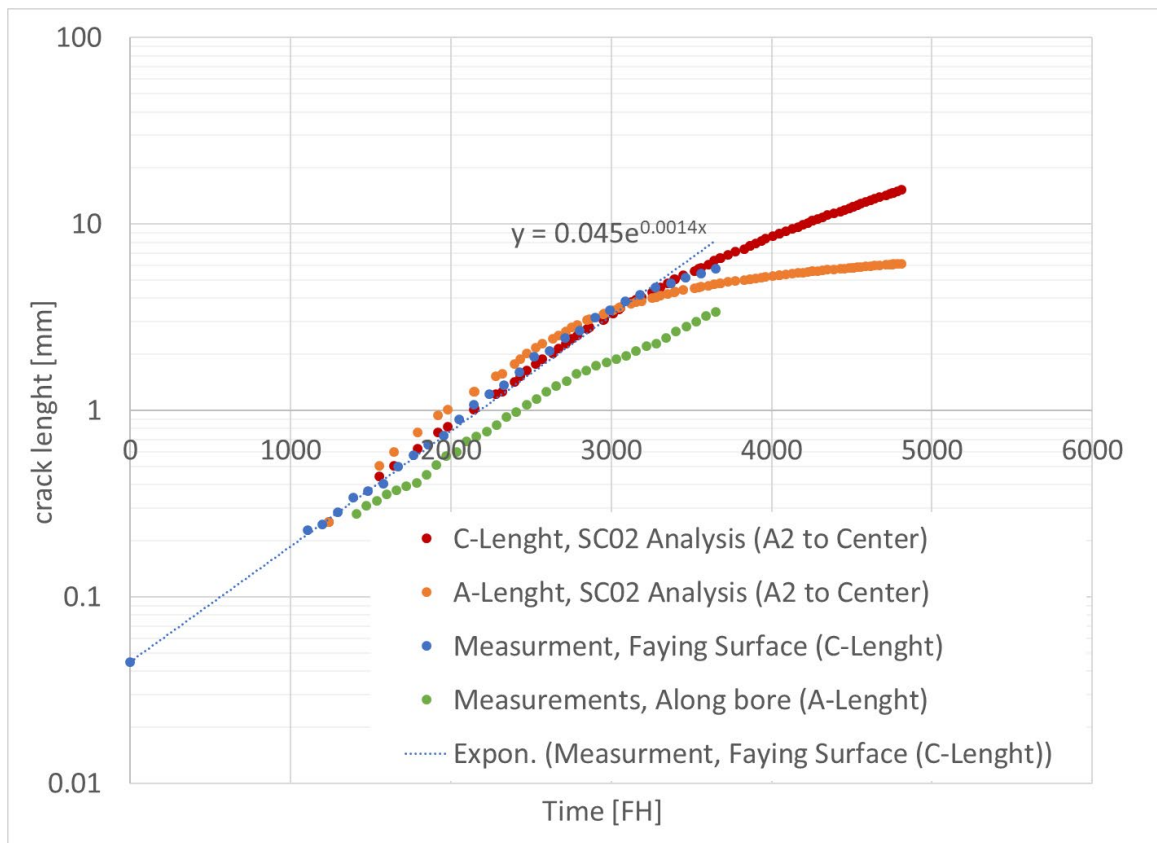


Figure 4. 18: AFGROW predictions vs. measurements, crack hole (A2) towards free center

For both scenarios, the prediction seems to be fairly accurate along the surface and slightly conservative along the bore.

For the scenario where a crack is growing towards the free edge of the TEF hinge, based on CG model results, it's expected that the crack will not break through the thickness until it becomes critical.

For the scenario where a crack is growing towards the hinge centerline, a similar behavior as the ones growing towards the free edge is obtained. The accuracy of the model is anyhow limited to small cracks. Once the crack has grown further away from the countersunk head, it could eventually start to accelerate again in the direction of the vertical flange that has not been accounted for in the CG model. That would require further assessment and additional QF data for calibration.

Anyhow, the obtained CG model are considered accurate enough for analysis purposes. Thus the obtained CG curves have been used as a basis to derive recurring inspection intervals for the Swiss F/A-18 fleet.

## **4.6 Fatigue Monitoring & Individual A/C Tracking based on Nz Exceedance Data**

RUAG AG, P. Mitropoulos, M. Rist, A. Uebersax

For fatigue monitoring, the Swiss Air Force F-5E/F are equipped with Fatigue Meters (FM) and an Electronic Structural Data Acquisition (ESDA) system. All F-5E are equipped with a Fatigue Meter, whereas all F-5F and 35% of the F-5E are equipped with an ESDA system. The Fatigue Meter records cumulative vertical acceleration (Nz) exceedances only, whereas the ESDA system records vertical and lateral accelerations, altitude and speed on a time-history basis.

The Swiss Air Force F-5E/F fleet fatigue monitoring was done by comparing the fleet average Nz exceedances to a cumulative exceedance curve of a reference spectrum that was used to calculate inspection intervals. From time to time, more specific usage investigations have been carried out, such as the Nz spectrum variation of individual aircraft and deviation from original mission and configuration mix. Some aircraft have been monitored as "individuals", especially aircraft used for the Patrouille Suisse, the Swiss Air Force Display Team.

As deviations from the assumed usage (mission, configuration and severity) became more frequent over the years, the need for a fleet-wide individual aircraft tracking grew, to ensure structural integrity of each separate aircraft. As the majority of the aircraft are equipped with FM, the approach was to find a solution based on cumulative exceedance data emanating from the FM readings.

The chosen approach takes the cumulative Nz exceedance data and reconstructs a pseudo-random time-history Nz sequence that is read into a crack initiation (CI) solver. By referencing the resulting CI live to the CI life of a reference spectrum, a Fatigue Usage Index (FUI) is calculated.

The chosen approach takes the cumulative Nz exceedance data and reconstructs a time-history sequence using an upper to lower curve excursion algorithm according to [2]. Several algorithms that have been proposed in [2] have been assessed:

- random peak through excursion (with and without logarithmic interpolation)
- random peak valley excursion
- upper to lower curve excursion
- extreme to extreme
- paired peak – valley

To evaluate the algorithms, cumulative exceedance spectra are processed from known Nz time-history sequences. These spectra are re-transformed into time-history sequences using the different algorithms. FUI values are calculated for each of these sequences and are compared to the FUI value of the reference time-history sequence. The upper to lower curve excursion algorithm revealed the best (robust, reproducible) results.

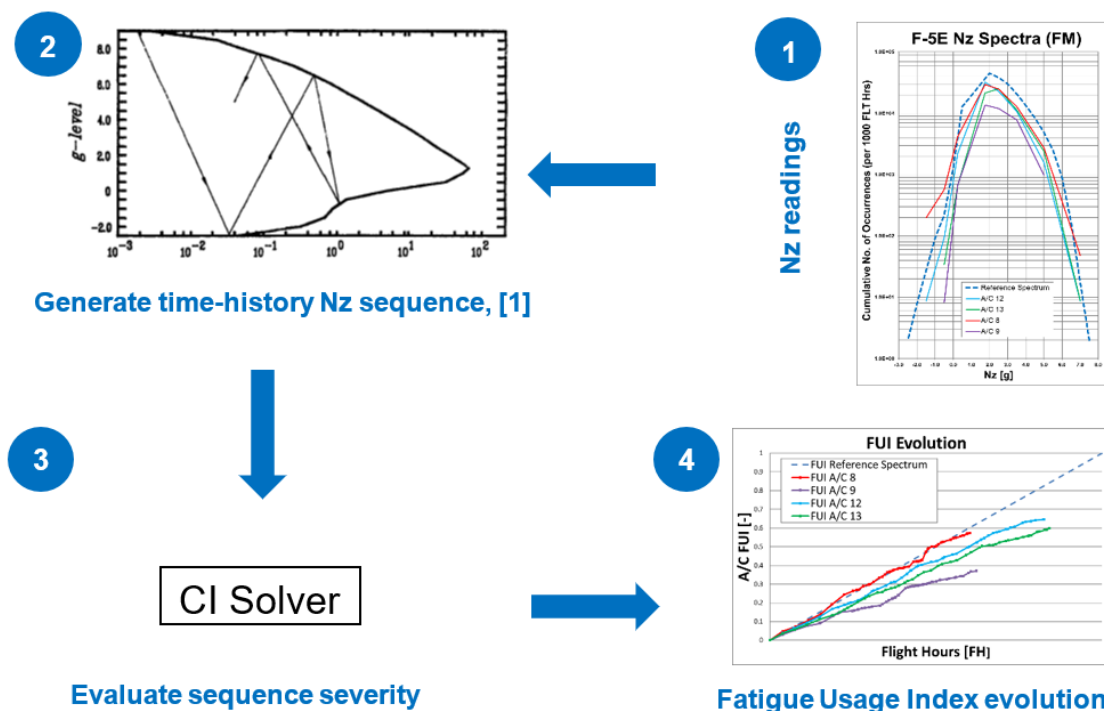


Figure 4. 19: Process of Fatigue Usage Index (FUI) calculation

<sup>2</sup> Ref.: Fatigue Life Under Random Load History Derived from Exceedance Curves using different Algorithms, Prakash et al,1993

Calculation of a Fatigue Usage Index (FUI):

$$\Delta FUI_i = \frac{\Delta t_i}{t_{cert}} \cdot \frac{CI Life_{ref}}{CI Life_i}$$

With  $\Delta t_i$  = reading period<sub>i</sub> between Nz exceedance readings

$t_{cert}$  = length of the certified service life

CI Life<sub>i</sub> = CI Life calculated with the spectrum from the reading period  $\Delta t_i$

CI Life<sub>ref</sub> = CI Life calculated with the reference spectrum

By summation of the FUI increments ( $\Delta FUI$ ), the FUI value at a specific point in time is obtained. The entire process is integrated in an analysis tool.

It was decided that the value FUI=1.0 is reached with the F-5E reference Nz spectrum after the certified service life, although other referencing concepts may be applied as well. Therefore, the reference stress used for the CI calculation is defined by the stress that results in the CI life = certified service life when run with the reference spectrum. For CI calculation the material values for the most common material used for the F-5E/F structure, i.e. aluminum alloy 7075-T73, is used.

F-5E Nz exceedance data is available since almost the very beginning of service in the Swiss Air Force. Missing data is substituted by reference spectra data.

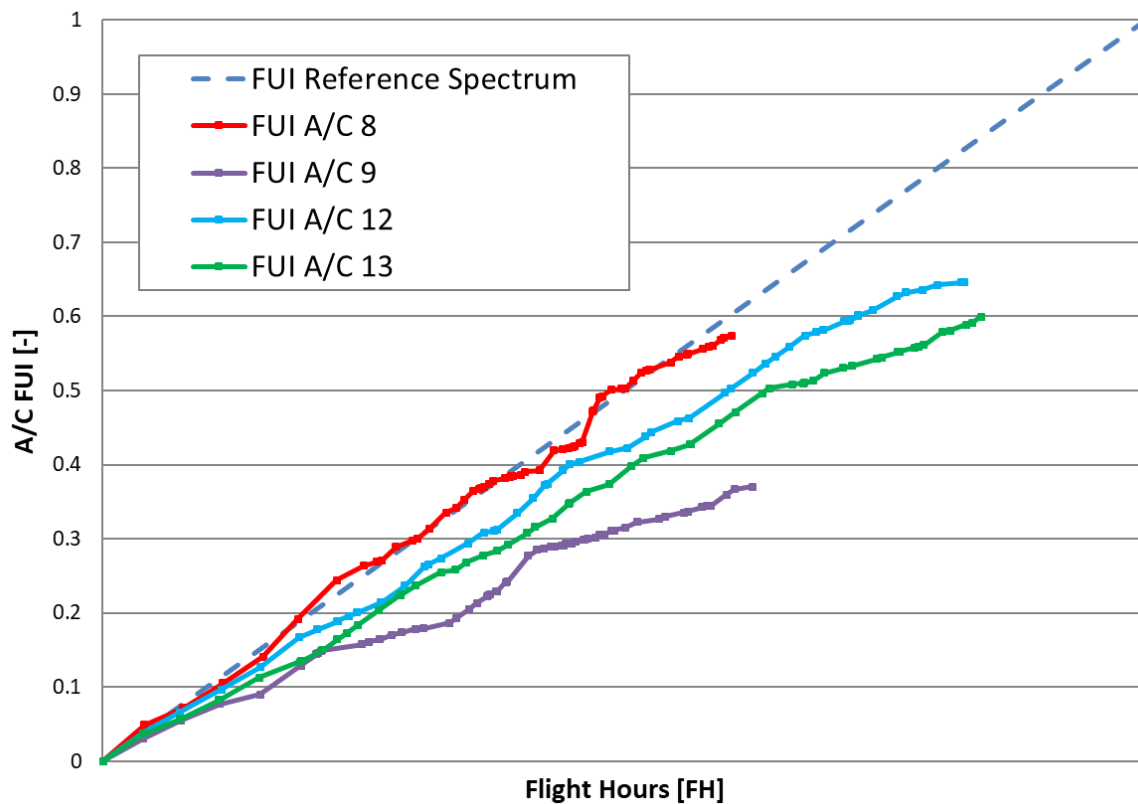


Figure 4. 20: FUI evolution of individual aircraft

It was shown that an effective individual aircraft tracking and fatigue monitoring could be set up, even with simple cumulative accelerometer exceedance data of existing legacy monitoring systems. The evaluation of the resulting FUI and FUI rate over the last years provides valuable inputs for fleet fatigue evaluation and control.

## 4.7 TSA Fatigue Evaluation

RUAG AG, E. Martins, I. Kongshavn

Due to possible future environmental regulation restrictions in the use of chromic acid substance, tartaric sulfuric acid anodizing (TSA) has been studied as a replacement for chromic acid anodizing (CAA), which is a surface treatment used in aluminium alloys that protects the material against corrosion, provides electrical insulation, improves paint adhesion and is used in components subject to high stress. Sulfuric acid anodizing (SAA) has also been studied as a reference.

The fatigue testing has been performed to verify that TSA does not have a more detrimental effect on fatigue life than the historically used CAA process at RUAG. The study compared the fatigue behaviour of sealed and unsealed TSA, CAA, SAA and raw materials by using a variable amplitude spectrum typical for fighter aircraft in both aluminium alloys AA7050-T451 plate and AA7075-T351 plate dog bone coupons with a low Kt geometry (6 coupons per test lot). A high and a low stress level were tested, which should result in a crack initiation (CI) life of approximately 6'000 flight hours and 18'000 flight hours. Constant amplitude marker bands were added to the spectrum to aid in post-test quantitative fractographic analysis of the crack growth.



Figure 4. 21: CAA sample, fracture surface after fatigue testing with many initiation origins at etch pits

The fatigue testing results revealed that the:

- Log average fatigue lives of the TSA coupons are the same or longer than those of CAA and SAA coupons;
- Raw material samples have a longer fatigue life compared to samples etched with CAA, SAA, and TSA, due to the absence of etch pits that facilitate crack initiation;

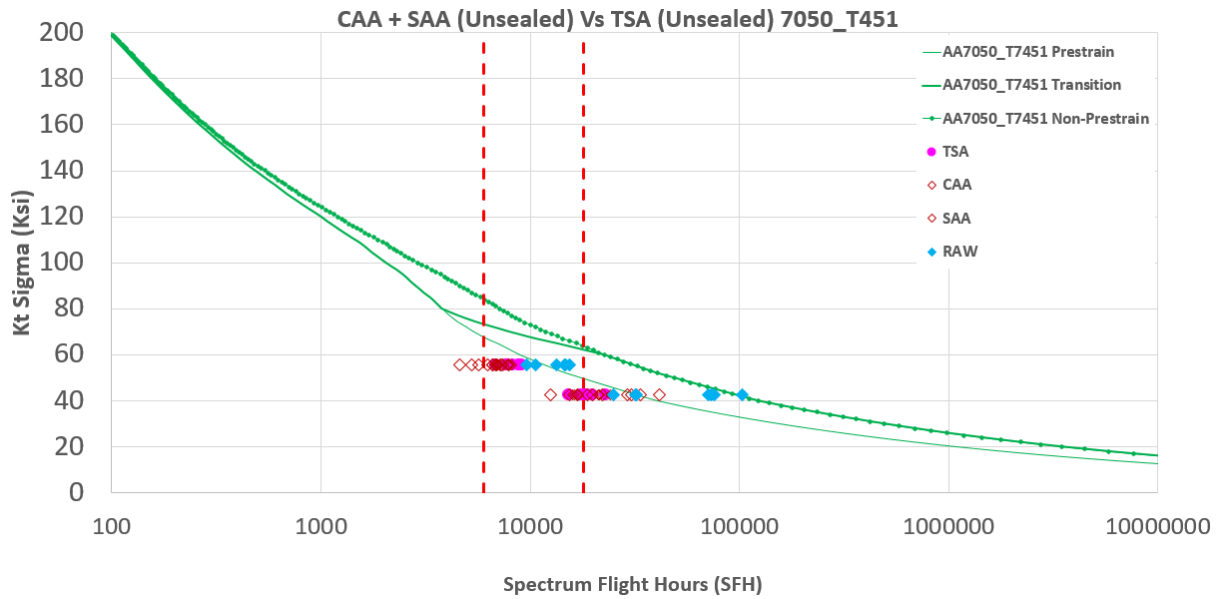


Figure 4. 22: Kt Sigma Vs Life - All unsealed 7050 Alloy samples comparison. The plotted CI life is assumed to be 2/3 of the total tested life, as measured by post-test quantitative fractography. TSA coupons have in general less scatter and are the same or longer than those of CAA and SAA.

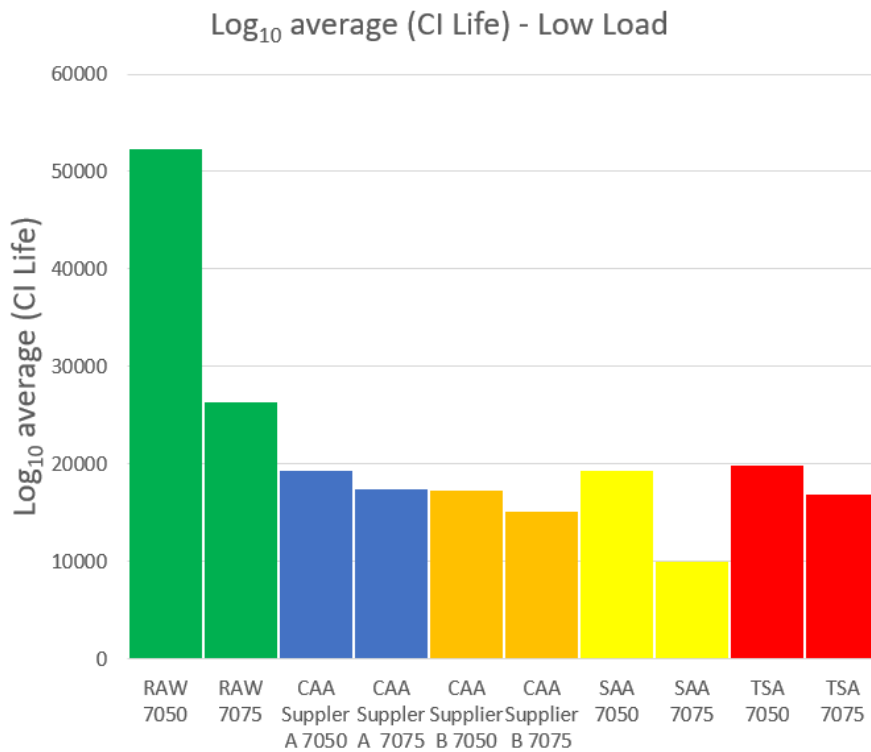


Figure 4. 23: Log<sub>10</sub> average values of CI Life - Low load. The CI life is assumed to be 2/3 of the total tested life. Log<sub>10</sub> average CI Life of TSA is higher or the same when comparing to CAA and SAA.

Quantitative fractography (QF) has also been performed in order to evaluate the crack growth rate in a selection of coupons to:

- Verify that the cause of crack initiation in etched samples was from etch pits, rather than from material anomalies such as interstitials or porosity, or from surface defects from the manufacturing;
- Investigate the cause of failure in the raw coupons, which had a much longer fatigue life;
- Measure the ratio of the crack initiation phase and crack growth phase.

Quantitative fractography (QF) results revealed:

- In the etched coupons, cracking initiates at relatively large etch pits, which can be up to 0.1 mm deep;
- The orientation of the coupons were chosen such that attack will occur preferably in the weakest T-L direction (load to crack growth orientation), in-between the grains;
- In the raw coupons, there is more scatter in the fatigue lives as crack initiation occurs at inclusions rather than readily available etch pits;
- TSA and CAA coupons had the thinnest anodized layer, of roughly equal magnitude In contrast, the SAA coupons had a very thick and consistent coating thickness;
- Assuming a 2/3 rule of thumb for the ratio of CI life to total life was confirmed by a QF evaluation of selected coupons.

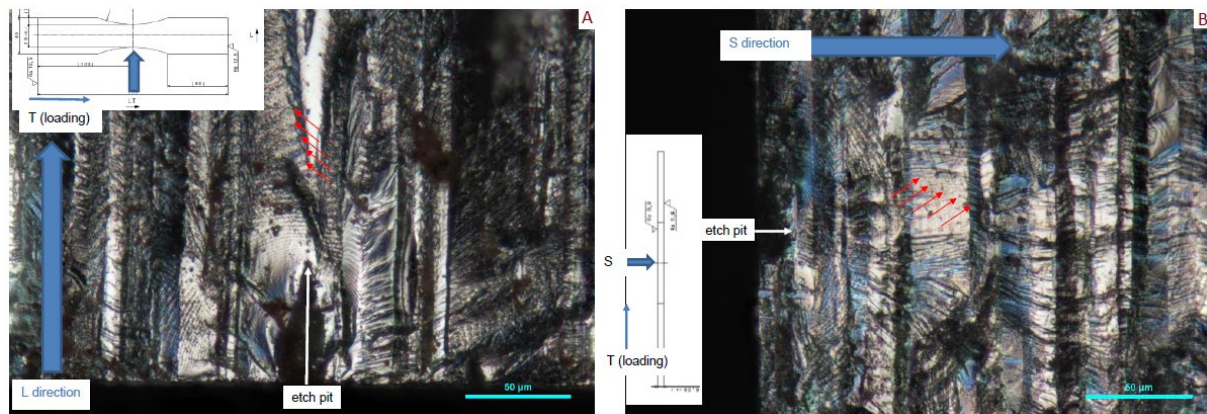


Figure 4. 24: A - Etch pit in the L direction in a CAA unsealed coupon. B - Etch pit in the S direction in a CAA sealed coupon. The red arrows represent a selection of crack fronts marked by the spectrum marker bands.

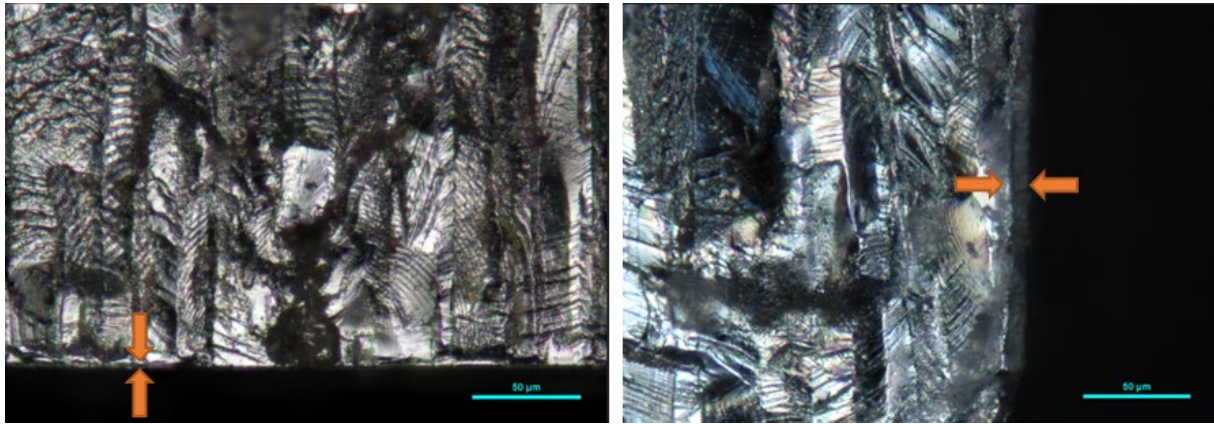


Figure 4. 25: Anodized layer of a TSA coupon (left) and the anodized layer of an SAA coupon (right)

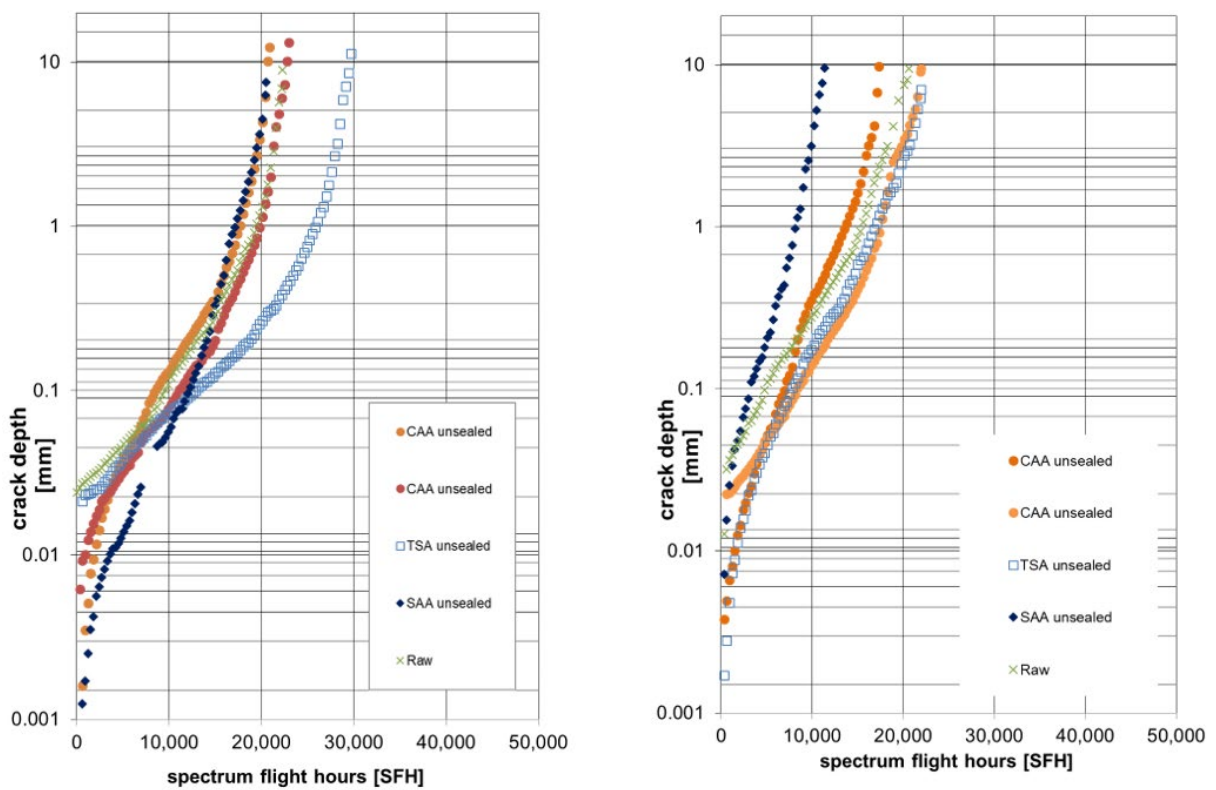


Figure 4. 26: QF curves for unsealed AA7050 (left) and AA7075 (right) for the low load level, collapsed such that all curves begin at zero flight hours to compare the crack growth rates (slopes).

The crack growth rates (slopes) are similar for the different surface treatments and the raw coupons in each material. The crack growth rates appear to be slightly higher in the AA7050 samples than in the AA7075 at this low load level. The samples shown were randomly selected for each surface treatment type and do not represent a general comparison of the fatigue lives.

In conclusion, for the surface treatment processes used in this test campaign, the TSA treatment has a similar effect on fatigue as the CAA process.

## 4.8 Development and operation of two test benches for the evaluation of a structural health monitoring system

Empa - Materials Science and Technology, Silvain Michel

### Introduction

In the Clean Sky 2 Joint Undertaking Innovation Action project DIMES, a fully integrated measurement system for structural health monitoring is being developed and evaluated. For the demonstration of such a system, typical structural parts had to be prepared, installed and loaded in a test environment. The project team identified two types of structural components, which were made available by the topic manager at Airbus for this purpose: An outer wing box of an Airbus A-320 and panels representing the fuselage of an A-350. While the wing box represents a classical metallic structure, the fuselage panels represent modern composite constructions.

The aim of the test bench task was to design, build and operate two test benches for these specimens and to simulate the loading of them as in a full-scale fatigue test. The Mechanical Systems Engineering Laboratory of Empa was charged with this task. The laboratory facilities were suitable for the construction and operation of these large component tests.

### The wing box test bench

The wing box (see Figure 4. 27) was approx. 5.4 meter long and 1.1 meter wide. It was the section between rib 18 and 27 of a left wing of an A-320-200. The wing box was pre-damaged, because it was from a crashed aircraft. It was repaired in the region where the front spar was broken due to the impact during the accident. The typical loads on this specimen were estimated with the following assumptions: mass of the aircraft of 85'000 kg, vertical acceleration 2 g, lift of one wing is 35% of the total lift, and lift of the outer wing section is 25% of the total wing lift. With these assumptions, the loading was estimated to be a vertical force of 250 kN and a bending moment of approximately 260'000 Nm at rib 18. Due to local restrictions on the introduction of the load, the bending moment applied was limited to 180'000 Nm. The wing section was clamped at each end by wood blocks and the load was applied with a servo-hydraulic actuator to the clamp at the tip end while the other end was fixed to the strong floor, see Figure 4. 28. The applied load was distributed over two ribs in the wing via the clamping arrangement. The test program consisted of constant amplitude and frequency cycling at different pre-load levels and a synthetic flight cycle program with variable amplitudes and frequencies, see Figure 4. 29. With this loading, it was expected, that at various locations in the front spar fatigue cracks would initiate and propagate.

### **The fuselage panel test bench**

The fuselage panels were also pre-damaged, because they were used in static component tests. They were 2.7 meter long and 1.1 meter wide. The fuselage panels had broken stringers and large delaminations between skin and stringers, see Figure 4. 30. It was decided to load the specimen under longitudinal compression and torsion. This loading regime was chosen in order to grow pre-existing delaminations. Three actuators were integrated in the test set-up: one for the compression load and two for the torsion load via a clamping arrangement at one end of the panel while the other end was fixed to the strong wall. The test setup is shown in Figure 4. 31.

### **Results and outlook**

While the wing box test has been completed, the fuselage panel test is still on going. During the constant amplitude and frequency loading of the wing box, fatigue cracks were propagated from a pre-existing crack in the front spar. The capability of the structural health monitoring system to detect and measure the growth of such typical cracks was evaluated. Results from the fuselage panel test are expected in the next weeks.

### **Conclusions**

Two test benches were successfully designed, built and operated to serve as a platform for the development and evaluation of a structural health monitoring system. With this task, the Mechanical Systems Engineering Lab was able to contribute to the DIMES project.

### **Acknowledgment**

The DIMES project has received funding from the Clean Sky 2 Joint Undertaking under the European Union's Horizon 2020 research and innovation program under Grant Agreement No 820951. This paper reflect only the author's view, and the Clean Sky 2 Joint Undertaking is not responsible for any use that may be made of the information it contains.

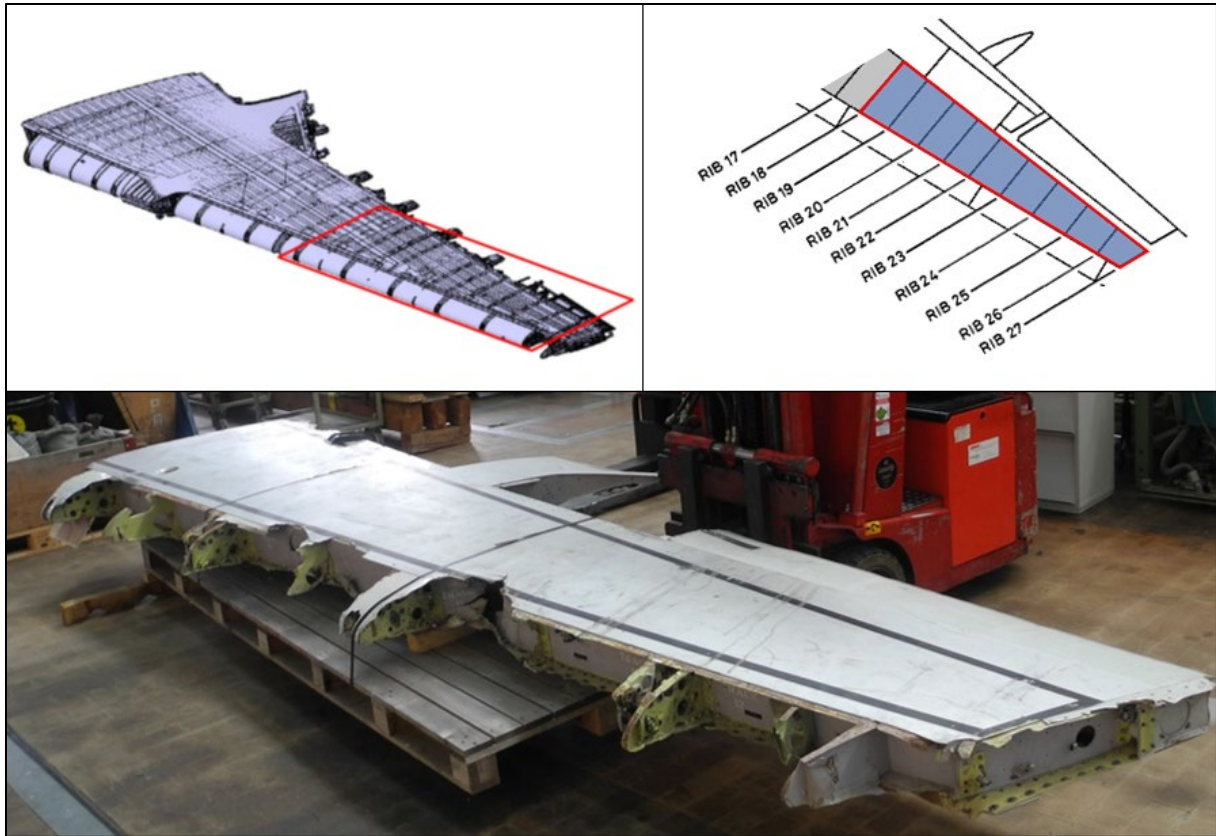


Figure 4. 27: First test specimen: Outer wing box from a crashed A-320-200 aircraft

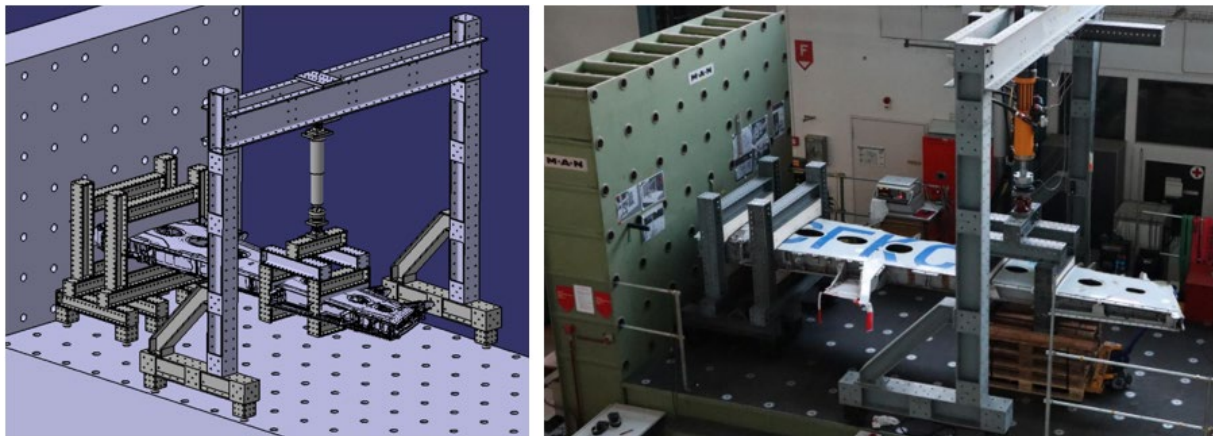


Figure 4. 28: Wing test bench at Empa: virtual set-up (left) and realization (right)

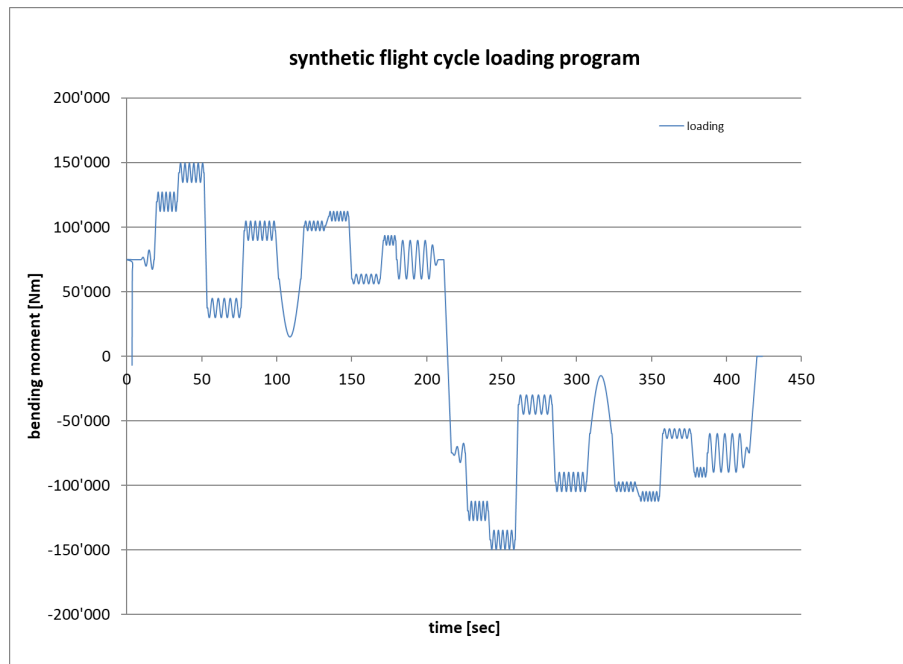


Figure 4. 29: Synthetic flight cycle loading program for the wing and fuselage test



Figure 4. 30: Second test specimen: Fuselage composite panels from an A-350 static test

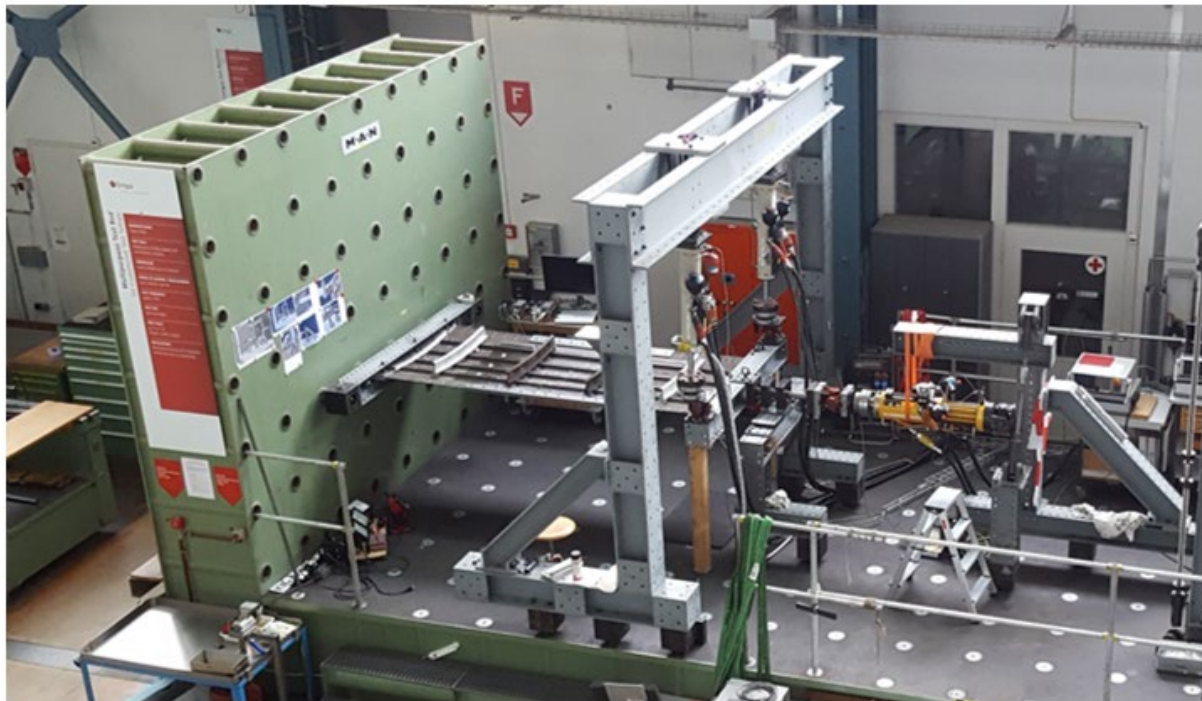
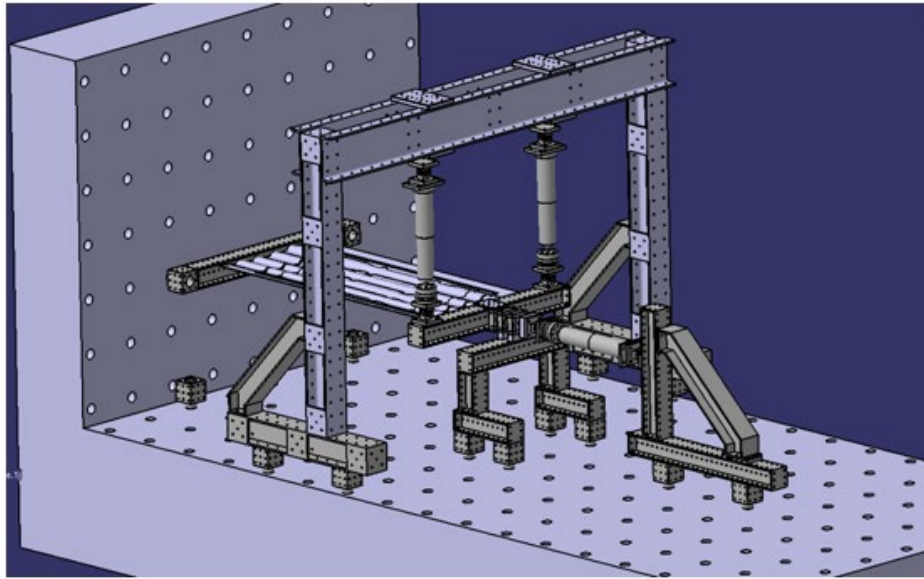


Figure 4. 31: Fuselage composite panel test bench at Empa: virtual set-up (top) and realization (bottom)